

Inversion domains in GaN layers grown on (111) silicon by molecular-beam epitaxy

A. M. Sánchez, F. J. Pacheco, S. I. Molina, and R. Garcia

Departamento de Ciencia de los Materiales e Ingeniería Metalúrgica y Química Inorgánica, Universidad de Cádiz, 11510 Puerto Real, CÁDIZ, Spain

P. Ruterana^{a)}

ESCTM-CRISMAT UMR CNRS, Institut des Sciences de La Matière et du Rayonnement, 6 Boulevard du Maréchal Juin, 14050 CAEN Cedex, France

M. A. Sánchez-García and E. Calleja

Departamento de Ingeniería Electrónica, ETSI Telecomunicación, Universidad Politécnica, 28040 Madrid, Spain

(Received 13 December 2000; accepted for publication 2 March 2001)

Transmission electron microscopy is used to investigate GaN layers grown on Si(111) substrates by plasma-assisted molecular-beam epitaxy. These layers were grown on top of different AlN buffer layers. Multiple-beam dark-field techniques applied to both cross-sectional and planar-view samples show the presence of inversion domains. These domains grow directly from the interface with the Si(111) substrate. Such observations are related, as in the case of growth on sapphire, to the symmetry difference between wurtzite and diamond. © 2001 American Institute of Physics.

[DOI: 10.1063/1.1368373]

Due to the increasing importance of nitride-based III-V materials, a large amount of research is being carried out for optimizing the growth, and to understand the structural defect effect on their optoelectronic properties. GaN films have been fabricated on a number of substrates such as sapphire with different crystallographic orientations,^{1,2} 6H-SiC,³ GaAs,⁴ and Si.⁵ The most successful devices until now are based on GaN layer grown over (0001) surface sapphire by metalorganic chemical vapor deposition (MOCVD). GaN layers containing large densities of dislocations and extended defects, approximately six orders of magnitude higher than what is acceptable for more conventional semiconductors, are used to fabricate devices.⁶ Dislocations, stacking faults,⁷ inversion domains⁸ (IDs), and nanotubes⁹ have been observed in the active GaN layers.

The epitaxial growth of GaN on Si is of great interest due to the well known Si technology and the potentially good opportunity to combine optoelectronics to the high integration of circuits. Moreover, the availability of large and high quality Si substrates, as well as its low cost, make it an attractive alternative for the growth of III-nitride layers. The Si(111) substrate presents the required hexagonal symmetry. However, the growth of GaN directly on Si(111) presents several difficulties due to the large lattice mismatch, the difference of thermal expansion coefficient, as well as surface chemistry. Nevertheless good GaN layers have been obtained using a buffer layer such as AlN^{10,11} or SiC.¹²

Microstructural characterization of GaN heteroepitaxy on Si(111) has received less attention although several studies by transmission electron microscopy have been performed for films grown by MOCVD and molecular-beam epitaxy (MBE).^{13,14} The GaN layers grown over Si(111) pos-

sess a typical threading dislocation distribution due to the misorientation between adjacent subgrains.¹³ Planar defects¹⁴ and nanotubes¹³ have also been observed. In previous articles, investigations of inversion domains have been carried out in GaN layers grown on sapphire;¹⁵⁻¹⁷ on SiC, the inversion domains were possibly due to the presence of an amorphous layer on top of the SiC substrate.⁹

In this work a detailed investigation has been carried out in GaN films grown on Si(111) by MBE using transmission electron microscopy (TEM). These layers contain a large amount of columnar domains which grow directly from the Si surface and we identify them as inversion domains.

GaN films have been grown by plasma-assisted MBE on Si(111) on axis substrates. In order to avoid amorphous Si-N formation and reduce the mismatch between GaN and Si(111) substrate, an AlN buffer layer has been grown. In the investigated samples, GaN was grown on the top of AlN buffer layers. A detailed report of the growth conditions can be found in Ref. 18.

Cross-sectional (XTEM) and planar-view (PVTEM) transmission electron microscopy samples were prepared by the conventional method, thinning down to 100 μm by mechanical grinding followed by dimpling down to 20 μm . Ion milling at 4.5 kV was used to achieve electron transparency. Conventional TEM studies using XTEM and PVTEM orientations were carried out on a Jeol 1200EX transmission electron microscope operating at 120 kV. High resolution electron microscopy studies were carried out on a Jeol 2000EX transmission electron microscope operating at 200 kV.

A bright field image recorded near the $[11\bar{2}0]$ zone axis is shown in Fig. 1 where several vertical domains are exhibited. This includes the mosaic structure with a high density of small misorientated subgrains as well as the inversion domains, if any. Therefore, we have carried out a detailed analysis of these samples along different zone axes.

^{a)}Author to whom all correspondence should be addressed; electronic mail: ruterana@ismra.fr

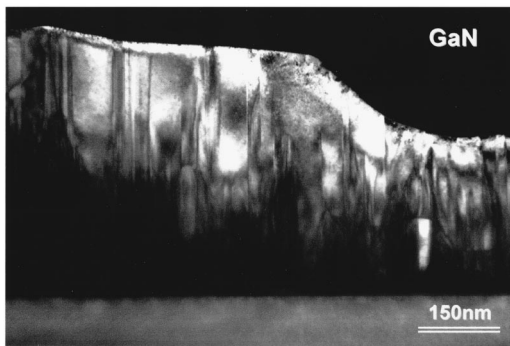


FIG. 1. Conventional bright field image taken near the $\langle 11\bar{2}0 \rangle$ zone axis.

Theoretical calculations carried out by Serneels *et al.*¹⁹ predict that under certain conditions, the inversion domain and the surrounding matrix should be different in contrast (i.e., a complementary contrast for $+g$ and $-g$ reflections). This technique had been previously used to determine inversion domains in GaN layers grown on sapphire.^{15,20} A non-centrosymmetric zone axis is necessary to achieve this characterization; $\langle 11\bar{2}0 \rangle$ zone axis has been used where $[000\bar{2}]$ direction of inverted domain is equivalent to the $[0002]$ direction in the matrix. Figure 2 shows images recorded under dark field multibeam conditions with $g=0002$ and $g=000\bar{2}$ reflections with the incident beam along a $\langle 11\bar{2}0 \rangle$ zone axis. A complementary contrast is observed in the images indicating that these domains are related to the surrounding matrix by an inversion operation.

In planar view, the same domains have been analyzed along the noncentrosymmetric $\langle 11\bar{2}3 \rangle$ zone axis. Multiple dark field imaging were recorded with $g=1\bar{1}01$ and $g=\bar{1}\bar{1}0\bar{1}$ [Figs. 3(a) and 3(b)]. The asymmetry between these two reflections has been used by Cherns *et al.*,¹⁷ in their study of inversion domains in GaN layers grown on sapphire. In PVTEM images of Figs. 3(a) and 3(b), a complementary contrast is observed with these two reflections, which means that inversion domains are present (*I*). However, the presence of nanotubes in the sample may lead to the wrong conclusions due to the similar contrast that both defects may present under specific reflections.¹⁶ Such tubes generally have a constant cross section, they are usually empty or filled with amorphous material. Along the *c* axis they exhibit a faceted and more or less hexagonal shape.¹⁶ Figure 3(c) shows the same area as in Figs. 3(a) and 3(b) along the $[0001]$ zone axis, no white contrast due to amorphous or empty nanopipes is present. From the comparison of the three images, it is clear that the investigated samples contain inversion domains.

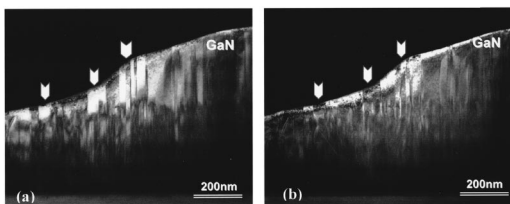


FIG. 2. Dark field images with (a) $g=0002$ and (b) $g=000\bar{2}$ in the $\langle 11\bar{2}0 \rangle$ zone axis. The opposite contrast shows inversion domains (arrows).

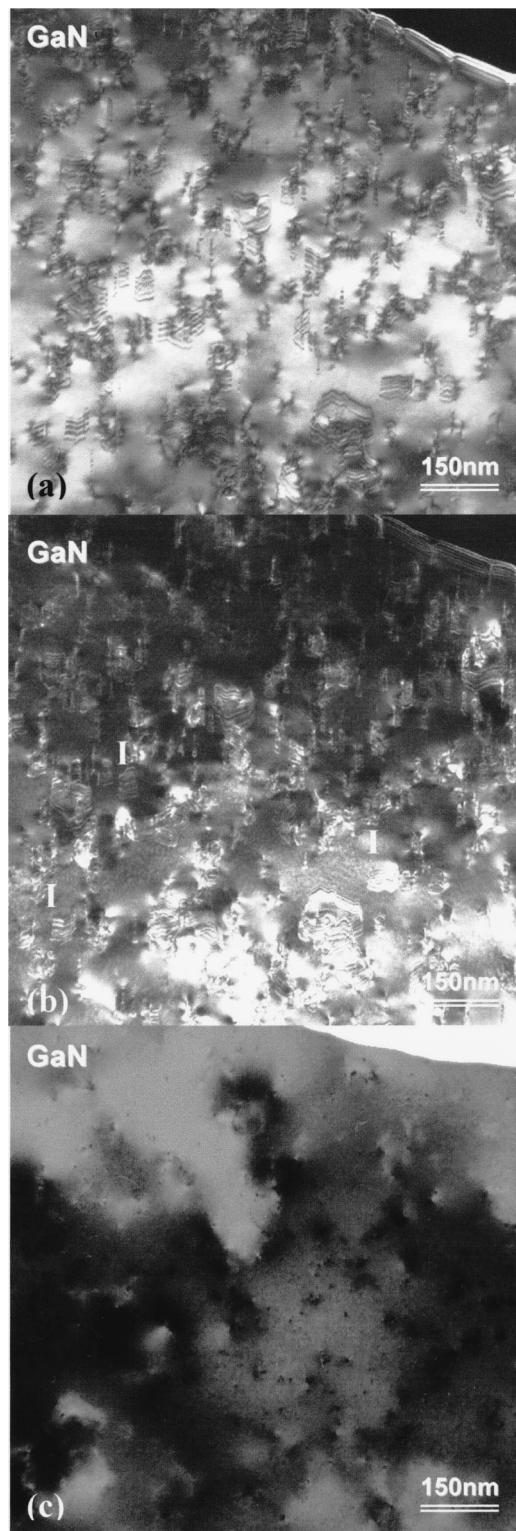


FIG. 3. Dark field images with (a) $g=1\bar{1}01$, (b) $g=\bar{1}\bar{1}0\bar{1}$, and (c) bright field image in $\langle 0001 \rangle$ zone axis showing inversion domains in the GaN layer, some of the domains are marked by white *I*'s.

In the $\langle 11\bar{2}0 \rangle$ HREM image of Fig. 4 an ID is observed to initiate on the silicon substrate. There is no amorphous layer at the interface with (111)Si. The domains present a smaller diameter at the interface with the silicon, they next take the typical columnar form, along the $[0001]$ direction in the GaN epilayer. The IDs origin is related to the symmetry difference between AlN and Si. AlN and GaN are of wurtzite type hexagonal symmetry and are noncentrosymmetric,

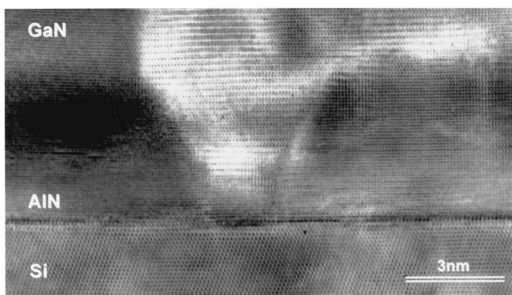


FIG. 4. HREM image taken in the $\langle 11\bar{2}0 \rangle$ zone axis showing the connection of inversion domain to the Si(111) substrate.

whereas the silicon substrate is cubic and centrosymmetric. This symmetry lowering across the interface explains the IDs formation inside the GaN layers.

In summary, inversion domains were characterized in GaN films grown over the Si(111) substrate by plasma-assisted MBE. The inversion domains' existence has been demonstrated in both cross section and planar view orientations using techniques described in previous GaN/sapphire work.^{17,20} The domains were found to originate directly from the substrate surface, like in the layers grown on sapphire.²¹ The generation of IDs can probably be explained by the difference between the symmetries of the materials involved. Both silicon and sapphire are centrosymmetric, whereas GaN and AlN are not. On sapphire, it was recently shown that the occurrence of inversion domain boundaries may be related to surface steps.²¹ Work is currently going on in order to determine the exact connection of these domains to the Si surface.

This work has been supported by CICYT Project No. MAT98-0823-C03-02 and Junta de Andalucía (Group No. PAI TEP 0120). One of the authors (P.R.) acknowledges the support of the EU under Contract No. HPRN-CT-1999-00040.

- ¹T. Sasaki and S. Zembatsu, *J. Appl. Phys.* **61**, 2533 (1987).
- ²C.-J. Sun and M. Razeghi, *Appl. Phys. Lett.* **63**, 973 (1993).
- ³B. N. Sverdlov, G. A. Martin, H. Morkoç, and D. J. Smith, *Appl. Phys. Lett.* **67**, 2063 (1995).
- ⁴S. Fujieda and Y. Matsumoto, *Jpn. J. Appl. Phys., Part 2* **30**, L1665 (1991).
- ⁵T. Lei, T. D. Moustakas, R. J. Graham, Y. He, and S. J. Berkowitz, *J. Appl. Phys.* **71**, 4933 (1992).
- ⁶S. D. Lester, F. A. Ponce, M. G. Craford, and D. A. Steigerwald, *Appl. Phys. Lett.* **66**, 1249 (1995).
- ⁷P. Vermaut, P. Ruterana, and G. Nouet, *Philos. Mag. A* **76**, 1215 (1997).
- ⁸V. Potin, P. Ruterana, and G. Nouet, *J. Appl. Phys.* **82**, 2176 (1997).
- ⁹Z. Liliental-Weber, H. Sohn, N. Newman, and J. Washburn, *J. Vac. Sci. Technol. B* **13**, 1578 (1995).
- ¹⁰P. Kung, A. Saxler, X. Zhang, D. Walker, T. C. Wang, I. Ferguson, and M. Razeghi, *Appl. Phys. Lett.* **66**, 2958 (1995).
- ¹¹M. A. Sanchez-Garcia, E. Calleja, F. J. Sanchez, F. Calle, E. Monroy, D. Basak, E. Muñoz, C. Villar, A. Sanz-Hervas, M. Aguilar, J. J. Serrano, and J. M. Blanco, *J. Electron. Mater.* **27**, 276 (1998).
- ¹²T. Takeuchi, H. Amano, K. Hiramoto, N. Sawaki, and I. Akasaki, *J. Cryst. Growth* **115**, 634 (1991).
- ¹³D. M. Follstaedt, J. Han, P. Provencio, and J. G. Fleming, *MRS Internet J. Nitride Semicond. Res.* **4S1**, G3.72 (1999).
- ¹⁴S. I. Molina, A. M. Sanchez, F. J. Pacheco, R. Garcia, M. A. Sanchez-Garcia, F. J. Sanchez, and E. Calleja, *Appl. Phys. Lett.* **74**, 3362 (1999).
- ¹⁵L. T. Romano, J. E. Northrup, and M. A. O'Keefe, *Appl. Phys. Lett.* **69**, 2394 (1996).
- ¹⁶F. A. Ponce, D. Cherns, W. T. Young, J. W. Steeds, and S. Nakamura, *Mater. Res. Soc. Symp. Proc.* **449**, 405 (1997).
- ¹⁷D. Cherns, W. T. Young, M. Saunders, J. W. Steeds, F. A. Ponce, and S. Nakamura, *Philos. Mag. A* **77**, 273 (1998).
- ¹⁸T. Palacios, F. Calle, M. Varela, C. Ballesteros, E. Monroy, F. B. Naranjo, M. A. Sanchez-Garcia, E. Calleja, and E. Munoz, *Semicond. Sci. Technol.* **15**, 996 (2000).
- ¹⁹R. Serneels, M. Snykers, P. Delavignette, R. Gevers, and S. Amelinckx, *Phys. Status Solidi B* **58**, 277 (1973).
- ²⁰V. Potin, G. Nouet, and P. Ruterana, *Philos. Mag. A* **79**, 2899 (1999).
- ²¹P. Ruterana, V. Potin, B. Barbaray, and G. Nouet, *Philos. Mag. A* **80**, 937 (2000).